The Mechanism of Stereospecific C−H Oxidation by Fe(Pytacn) Complexes: Bioinspired Non-Heme Iron Catalysts Containing cis-Labile Exchangeable Sites**

Irene Prat,[a] Anna Company,*[a] Verònica Postils,[a] Xavi Ribas,[a] Lawrence Que, Jr.,[b] Josep M. Luis,*[a] and Miquel Costas*[a]

Abstract: A detailed mechanistic study of the hydroxylation of alkane C−H bonds using H_2O_2 by a family of mononuclear non heme iron catalysts with the formula $[Fe^{II}(CF_3SO_3)_2(L)]$ is described, in which L is a tetradentate ligand containing a triazacyclononane tripod and a pyridine ring bearing different substituents at the α and γ positions, which tune the electronic or steric properties of the corresponding iron complexes. Two inequivalent cis-labile exchangeable sites, occupied by triflate ions, complete the octahedral iron coordination sphere. The C−H hydroxylation mediated by this family of complexes takes place with retention of configuration. Oxygen atoms from water are incorporated into hydroxylated products and the extent of this incorporation depends in a systematic manner on the nature of the catalyst, and the substrate. Mechanistic probes and isotopic analyses, in combination with detailed density functional theory (DFT) calculations, provide strong evidence that C−H hydroxylation is performed by highly electrophilic $[Fe^V(O)(OH)L]$ species through a concerted asynchronous mechanism, involving homolytic breakage of the C−H bond, followed by rebound of the hydroxyl ligand. The $[Fe^V(O)(OH)L]$ species can exist in two tautomeric forms, differing in the position of oxo and hydroxide ligands. Isotopic-labeling analysis shows that the relative reactivities of the two tautomeric forms are sensitively affected by the α substituent of the pyridine, and this reactivity behavior is rationalized by computational methods.

Keywords: bioinorganic chemistry · density functional calculations · non-heme iron · oxidation · reaction mechanisms

Introduction

The selective oxidation of hydrocarbons in general, and alkanes in particular, remains a challenge of major interest in chemistry.[1] The direct transformation of a sp³ C−H bond into a functionalized C−O bond in a selective fashion could lead to new, shorter, and more straightforward strategies for the synthesis of complex organic molecules. Besides its magnificent potential significance in organic synthesis, oxidation of unactivated C−H bonds also represents a formidable fundamental chemica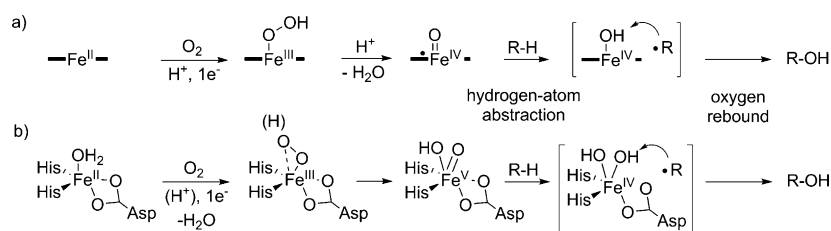l challenge that has fascinated chemists from a variety of fields. Although the total oxidation of hydrocarbons into CO_2 and H_2O is a thermodynamically favored process, alkyl C−H bonds are very strong and nonpolar; consequently, their functionalization has kinetic barriers that render these bonds as inert. Highly reactive catalysts are needed to overcome this inert character, and particularly interesting are those that can lead to selective C−H oxidation by using environmentally friendly oxidants (e.g., O_2 or H_2O_2).[2] Along this line, iron is a particularly interesting metal for the development of catalysts because it is inexpensive, highly abundant, and non-toxic.[1b,3] Thus, the combination of iron and clean oxidants for the performance of selective sp³ C−H oxidations is regarded as a highly desirable objective in modern synthetic chemistry.

In spite of the inherent difficulty in achieving this targeted objective, selective C−H oxidation is routinely carried out in biology; a number of enzymes perform such transformations under very mild conditions using iron as the metal center and O_2 as the terminal oxidant, which usually occurs by its reductive activation upon binding to a ferrous site(s). Prominent examples are heme (e.g., cytochromes P450)[4] and mononuclear non-heme iron enzymes (e.g., Rieske oxygenases).[5] Cytochromes P450 serve as the paradigm of O_2 activation and C−H oxidation by iron enzymes and they have been thoroughly studied (Scheme 1).[4,6] C−H bond hydroxylation is carried out by an oxo-iron(IV) porphyrin radical

[a] I. Prat, Dr. A. Company, V. Postils, Dr. X. Ribas, Dr. J. M. Luis, Dr. M. Costas
Institut de Química Computacional i Catàlisi (IQCC)
Departament de Química, Universitat de Girona
Campus Montilivi, 17071 Girona (Spain)
E-mail: anna.company@udg.edu
josepm.luis@udg.edu
miquel.costas@udg.edu

[b] Prof. L. Que, Jr.
Department of Chemistry, University of Minnesota
207 Pleasant St, SE, Minneapolis, 55455 MN (USA)

[**] Pytacn = 1-(2-pyridylmethyl)-4,7-dimethyl-1,4,7-triazacyclononane.

⌨ Supporting information for this article is available on the WWW under http://dx.doi.org/10.1002/chem.201300110.

Scheme 1. Mechanistic proposals for the formation of formally iron(V)-oxo oxidants in biological systems and the rebound mechanism for alkane hydroxylation. a) Cytochrome P450; b) Rieske oxygenases.

cation (Porph$^{+\cdot}$Fe^{IV}=O) through the so-called "rebound mechanism". This mechanism was first proposed by Groves et al.[7] and it consists of a stepwise process with two parts: 1) hydrogen-atom abstraction from the C−H bond by the oxo group to form an alkyl radical and a metal-hydroxo moiety, and 2) interaction of the radical with the newly formed hydroxo ligand to give the final hydroxylated species (oxygen-rebound). The capture of the alkyl radical must occur rapidly to account for the selectivity and stereospecificity observed in cytochrome P450 enzymes.[6a–c]

Rieske oxygenases can be considered as the non-heme counterparts of cytochrome P450s and they catalyze an array of oxidative transformations even more diverse than those associated with the heme systems.[5a–c,e] The iron center in these enzymes is coordinated to the so-called facial triad (two histidines and one carboxylate), in such a way that the metal coordination positions available for interaction with the substrate and/or the oxidant are disposed in a relative *cis* configuration. This feature contrasts with the *trans* disposition of the free sites found in heme enzymes. However, several studies suggest that the mechanism of action of Rieske oxygenases parallels that observed in heme enzymes. The main difference presumably lies in the nature of the high-valent iron-oxo species, which in the non-heme case is best described as a true oxo-iron(V) because of the lack of a redox non-innocent ligand such as the porphyrin. Indeed, indirect experimental evidence for the implication of Fe^{V}−oxo species in the catalytic cycle of Rieske dioxygenases has been obtained.[8] Most remarkably, it is proposed that the hydroxylation of C−H bonds follows the above-described rebound mechanism (Scheme 1b), which entails the formation of a transient alkyl radical. Experiments with radical clock substrate probes support this proposal by showing that short-lived carbon-centered radicals are formed during the oxidation reaction.[8b] Therefore, there is strong evidence that points to a common reaction mechanism operating in cytochrome P450 and in Rieske oxygenases.
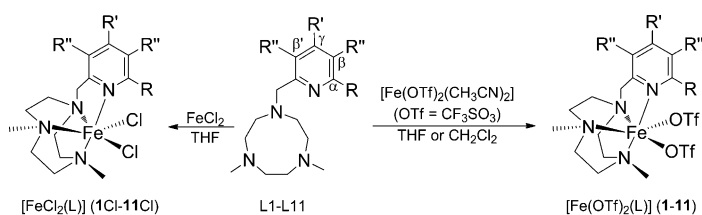
Whereas cytochrome P450 has inspired the development of porphyrin-based selective C−H oxidation catalysts,[6c,9] Rieske oxygenases constitute the biological precedent for exploring this reactivity at a mononuclear non-heme iron center.[10] This represents an attractive and challenging task as oxidation reactions with non-heme iron catalysts are vastly dominated by Fenton-type free-diffusing radical paths.[11] Nevertheless, in the last decade it has been proven

that selected non-heme iron catalysts can elicit enzyme-like metal-based C−H oxidation without the implication of free-diffusing radicals.[10–12] More recently some of these catalysts have emerged as powerful and unique synthetic tools in C−H oxidation reactions.[13]

A fundamental question that arises from these studies is the understanding of the mechanisms operating in non-heme iron-based C−H oxidation reactions, and the extent to which they overlap with those described for cytochrome P450s and synthetic heme systems. Mechanistic information about non-heme systems is scarce compared with their heme counterparts, the collection of which is usually hampered by the paramagnetic nature and high reactivity of the oxidizing species involved, which do not accumulate to a substantial extent.

We have previously shown that the non-heme coordination complex [Fe^{II}(CF$_3$SO$_3$)$_2$(Pytacn)] (**1**) (Scheme 2) catalyzes the hydroxylation of alkanes, as well as the epoxida-

ligand	L	R	R'	R''
Pytacn	L1	H	H	H
6Me-Pytacn	L2	Me	H	H
6Cl-Pytacn	L3	Cl	H	H
6F-Pytacn	L4	F	H	H
4Me-Pytacn	L5	H	Me	H
4Cl-Pytacn	L6	H	Cl	H
4NO$_2$-Pytacn	L7	H	NO$_2$	H
4NMe$_2$-Pytacn	L8	H	NMe$_2$	H
4CO$_2$Et-Pytacn	L9	H	CO$_2$Et	H
4OMe-Pytacn	L10	H	OMe	Me
4,6Me-Pytacn	L11	Me	Me	H

Scheme 2. Ligands and complexes used in this work.

tion and *cis*-dihydroxylation of olefins.[14] Several mechanistic probes indicate the involvement of a metal-based oxidant in these transformations. Therefore, this complex can be considered a functional model for the family of Rieske oxygenases. Very recently, experimental evidence for the involvement under catalytic conditions of a highly electrophilic [Fe^{V}(O)(OH)(Pytacn)]$^{2+}$ species was obtained by means of variable-temperature mass spectrometry (VT-MS), in combination with isotopic labeling, and density functional theory (DFT) calculations.[15] The involvement of oxo-

iron(V) species in catalytic C−H and C=C oxidation reactions had been previously inferred for this[14,16] and other non-heme iron catalysts on the basis of product analysis, isotopic analysis of reaction products using ^{18}O-labeled reagents (such as $H_2^{18}O$ or $H_2^{18}O_2$),[12a,17] DFT calculations,[18] kinetic studies,[19] EPR spectroscopy,[20] and mass spectrometry.[13b,21] In parallel to these studies, two examples of oxo-iron(V) complexes that could be fully spectroscopically characterized have been recently described.[22] On the other hand, experimental evidence has accumulated that this chemistry is highly sensitive to the nature of the ligands, and oxo-iron(IV) species may be responsible for oxidations in specific families of complexes.[23]

Taking these precedents into consideration, we go a step further in the present work and obtain an insight into the mechanism by which $[Fe^V(O)(OH)(Pytacn)]^{2+}$ reacts with alkanes, that is, the fundamental nature of the "oxygen-rebound" mechanism in a non-heme model complex. To do so, we have used isotopic analysis and computational methods to study the mechanism of C−H bond hydroxylation mediated by a family of complexes in which the tetradentate Pytacn ligand has been systematically modified with respect to its electronic and steric parameters. This family of complexes constitute a suitable platform to investigate how these parameters affect the C−H oxidation reaction, providing a detailed fundamental understanding on the C−H cleavage and C−O bond formation events at a non-heme site. Results disclosed in this work serve as the basis for understanding the mechanism by which C−H bonds are hydroxylated at a non-heme iron center containing *cis*-labile sites.

Results and Discussion

Chemical diversity of the [Fe(Pytacn)] family of catalysts: Pytacn-based ligands incorporating systematic modifications in the pyridine ring (Scheme 2) were targeted and the corresponding iron(II) triflate complexes $[Fe^{II}(CF_3SO_3)_2L]$, L = L1–L11 (compounds **1–11**) were prepared and characterized. Compounds **1** and **2** have been reported before,[14] and full details corresponding to the spectroscopic and structural properties of **3–11** will be reported elsewhere. In general terms, the substituents in the γ position of the pyridine ring (**5–11**) were introduced to tune the electronic properties of the pyridine so that such effects could be evaluated in their corresponding catalytic C−H oxidation reactivities. On the other hand, substitution in the sixth position of the pyridine (compounds **2–4** and **11**) was aimed at influencing the properties of the iron center both from an electronic and a steric point of view, because the groups at this position are located spatially close to the ligands occupying the two *cis*-labile exchangeable coordination sites.

To quantify the electronic effects exerted by the substituents introduced in the pyridine ring, the electrochemical potential ($E_{1/2}$) of the Fe^{III}/Fe^{II} redox pair was determined for the bis-chloro complexes $[Fe^{II}Cl_2L]$, in which L = L1, L2, L5–L11 (**1**Cl, **2**Cl, and **5**Cl–**11**Cl, see Table 1). Analogous
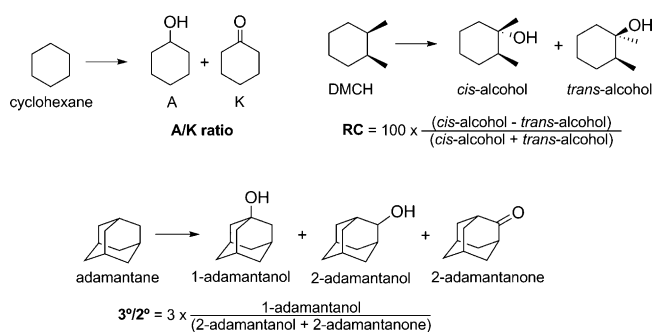
Table 1. Measured $E_{1/2}$ values (vs. SCE) for the Fe^{III}/Fe^{II} redox pair in **1**Cl, **2**Cl and **5**Cl–**11**Cl in CH_3CN.

Complex	$E_{1/2}$ [mV][a]
1Cl	138
2Cl	211
5Cl	176
6Cl	165
7Cl	225
8Cl	11
9Cl	171
10Cl	107
11Cl	238

[a] All cyclic voltammograms were recorded at a scan rate of 100 mV s^{-1}. The complexes were dissolved in previously degassed CH_3CN containing the necessary amount of n-Bu$_4$NPF$_6$ as supporting electrolyte to yield a 0.1 M ionic strength solution. All $E_{1/2}$ values were estimated as the average of the oxidative and reductive peak potentials ($E_{pa} + E_{pc}$)/2.

analyses with triflate complexes (**1–11**) were precluded by their chemically irreversible redox behavior. Cyclic voltammetry for **4**Cl, which contains a fluorine atom in the α position of the pyridine ring, showed multiple waves preventing direct measurement of the electrochemical potential. A direct comparison between the measured redox potentials reveals that the electronic properties of the γ substituent in the pyridine ring directly influence the redox potential of the iron center. For example, the highly electron-withdrawing NO$_2$ group (**7**Cl) causes an increase of the redox potential by 87 mV with respect to the unsubstituted system (**1**Cl, $E_{1/2} = 138$ mV vs. the saturated calomel electrode (SCE)). Instead, the introduction of the electron-donating NMe$_2$ group (**8**Cl) decreases the redox potential down to $E_{1/2} = 11$ mV. Subtler modifications of the $E_{1/2}$ values are observed with less-electron-donating or -withdrawing groups such as a chloride, an ester, or a methoxide functionality (**6**Cl, **9**Cl, or **10**Cl, respectively). The only exception to the predictable effect on the redox potential corresponds to **5**Cl bearing a methyl group in the pyridine γ-position, which affords a counterintuitive increase of the redox potential with respect to **1**Cl. In conclusion, the cyclic voltammetry (CV) experiments show that manipulation of the γ position of the pyridine ring of the Pytacn ligand platform translates into substantial changes in the electron density at the iron center without affecting the spatial properties of the *cis*-labile sites of the complexes.

Finally, the introduction of a methyl group in the α-position of the pyridine increases the redox potential by approximately 70 mV (compare **1**Cl vs. **2**Cl, and **5**Cl vs. **11**Cl) (Table 1). This effect can be understood by considering that the steric clash between the methyl group and the iron center disfavors the formation of the shorter Fe−N bonds of the iron(III) with respect to iron(II).[24] Therefore, manipulation of the α position of the pyridine influences not only the spatial properties of the nearby *cis*-labile sites, but also has an effect on the electron density at the iron site.

Scheme 3. Mechanistic substrate probes used to evaluate the involvement of metal-centered oxidants in C−H oxidation reactions. DMCH = cis-1,2-dimethylcyclohexane. For reaction conditions see footnote [a] in Table 2.

An efficient family of catalysts for C−H oxidation: The catalytic properties of **1–11** were tested in the hydroxylation of cyclohexane employing H_2O_2 as the oxidant (Scheme 3, Table 2).[14] In a typical experiment, hydrogen peroxide (10 equiv) diluted in acetonitrile was delivered by using a sy-

Table 2. Alkane hydroxylation reactions catalyzed by **1–11**.[a]

Catalyst	Cyclohexane A+K[b] (A/K)	KIE[c]	Adamantane 3°/2°[d]	DMCH RC [%][e]
1[14]	6.5 (12.3)	4.3	30	93
2[14]	7.6 (10.2)	3.4	20	94
3	6.8 (6.7)	3.3	28	88
4	5.9 (5.7)	4.5	19	86
5	6.5 (10.5)	5.0	30	88
6	5.9 (8.3)	4.3	30	94
7	5.3 (8.1)	4.3	29	89
8	4.3 (8.9)	4.9	23	94
9	5.7 (9.2)	4.1	28	94
10	6.2 (10.2)	4.2	23	95
11	6.1 (9.3)	4.0	15	95

[a] H_2O_2 (10 equiv) was delivered by a syringe pump to an acetonitrile solution containing the iron catalyst (1 equiv) and the substrate (10–1000 equiv). 1000 equiv substrate for cyclohexane and DMCH. 10 equiv for adamantane. [b] Turnover number (TON) (mol of product/mol of catalyst), A = cyclohexanol, K = cyclohexanone. [c] Kinetic isotope effect determined for cyclohexanol formation measured in the oxidation of a 1:3 mixture of cyclohexane/[D_{12}]cyclohexane. [d] 3°/2° ratio in adamantane oxidation = 3 × (1-adamantanol)/(2-adamantanol + 2-adamantanone). [e] Percentage of retention of configuration in the oxidation of the tertiary C−H bonds of cis-1,2-dimethylcyclohexane (DMCH) = (cis−$trans$)/(cis+$trans$) × 100.

ringe pump over a period of 30 min to an acetonitrile solution containing the iron catalyst (1 mM), cylohexane (1 M) and water (1 M). As previously shown for **1** and **2**,[14] under these conditions, complexes **3–11** afford efficient conversions (43–76 %, Table 2) of H_2O_2 into cyclohexanol and cyclohexanone products (Scheme 3). Comparison of these values with those obtained with related iron complexes under analogous experimental conditions[10,12a,23a,25] further reinforces the initial conclusions that the Pytacn ligand architecture gives rise to mononuclear iron complexes with remarkable catalytic activity.[14a] Compound **8** afforded the

lowest yields (turnover number (TON) of 4.3), suggesting that the NMe_2 group might be susceptible to oxidation, which, in turn, decreases the robustness of this catalyst.
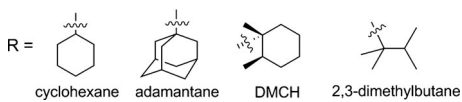
The oxidation of several mechanistic substrate probes (Scheme 3) was also studied to demonstrate the involvement of highly selective metal-centered oxidants in the present reactions.[11,26] Apart from the remarkably high [cyclohexanol]/[cyclohexanone] (A/K; A = cyclohexanol, K = cyclohexanone) ratio (5.7–12.3) found in the oxidation of cyclohexane, compounds **1–11** also exhibit selectivity parameters indicative of a metal-based oxidant (Table 2): relatively large kinetic isotope effects (KIE) were measured in the oxidation of a mixture of cyclohexane/[D_{12}]cyclohexane (1:3) (KIE values range from 3.4 to 5.0) and a high preference for the reaction with tertiary C−H bonds compared with secondary ones was found in the oxidation of adamantane (normalized 3°/2° = 15–30). Thus, the data clearly indicates that the strength of the C−H bond plays a major role in dictating the C−H site selectivity. Most remarkably, the oxidation of cis-1,2-dimethylcyclohexane (DMCH) catalyzed by complexes **1–11** showed a large degree of stereoretention clearly indicating that long-lived carbon-centered radicals or cations are not significantly involved in the C−H oxidation reaction. The high stereoretention in DMCH oxidation, large KIE values in the oxidation of cyclohexane, and normalized 3°/2° adamantane selectivities (Table 2) clearly differ from reactions initiated by hydroxyl radicals and they are indicative of the involvement of a highly selective metal-centered oxidant in these reactions.[11,26]

Isotope-labeling studies: To gain a deeper insight into the mechanism involved in the hydroxylation reactions, the origin of the oxygen atoms introduced into the alcohol product was established by means of isotopic-labeling experiments by using $H_2^{18}O_2$ or $H_2^{18}O$. Preliminary experiments performed by varying the concentration of $H_2^{18}O$ in the oxidation of cyclohexane with catalyst **1** indicated that oxygen atoms coming from water are incorporated into oxidation products, and the level of incorporation depends on [H_2O] (see Supporting Information, Table S1 and Figure S1).[14b] It increases linearly with [H_2O] at low concentrations, however a plateau is reached at higher concentrations, indicative of a saturation behavior. This behavior is characteristic of a pre-equilibrium involving reversible water-binding at the iron catalyst.[12a] The data indicated that 1000 equiv of water afforded saturation conditions, above which the percentage of water incorporated remained approximately constant. For this reason we fixed 1000 equiv of water as the amount employed in our experimental conditions.

Complexes **1–11** (1 equiv) were used as catalysts for the oxidation of cyclohexane (1000 equiv) with $H_2^{18}O$ (1000 equiv) and non-labeled H_2O_2 (10 equiv) as the oxidant. In all cases, significant levels of oxygen from water were incorporated into cyclohexanol (Table 3). However, depending on the catalyst used, the level of water incorporation varied significantly from 50 to 11 %. For selected complexes, complementary experiments performed by using

Table 3. Percentage ^{18}O incorporation into alcohol products by catalysts **1–11** in the presence of $H_2^{18}O$ or $H_2^{18}O_2$.[a]

R = cyclohexane   adamantane   DMCH   2,3-dimethylbutane

	Labeling source	Substrate [equiv]	Percentage ^{18}O incorporation for catalysts										
			1	**2**	**3**	**4**	**5**	**6**	**7**	**8**	**9**	**10**	**11**
cyclohexane	$H_2^{18}O_2$[b]	1000	47	85	–	63	48	–	–	–	–	–	76
	$H_2^{18}O$[c]	1000	45	11	28	24	39	47	50	36	48	44	13
	mass balance[d]		92	96	–	87	87	–	–	–	–	–	89
adamantane	$H_2^{18}O$[c]	10	74	3	–	11	72	–	–	–	–	–	2
DMCH	$H_2^{18}O$[c]	1000	79	2	14	10	65	70	66	68	72	72	3
	$H_2^{18}O$[c]	50	83	1	–	11	69	–	–	–	–	–	4
2,3-dimethylbutane	$H_2^{18}O$[c]	1000	76	1	–	4	72	–	–	–	–	–	1

[a] H_2O_2 (10 equiv) and H_2O (1000 equiv) were delivered by syringe pump to an acetonitrile solution containing the iron catalyst (1 equiv) and the substrate (10–1000 equiv). [b] Percentage of ^{18}O-labeled alcohol in the presence of 10 equiv $H_2^{18}O_2$ and 1000 equiv H_2O. [c] Percentage of ^{18}O-labeled alcohol in the presence of 10 equiv H_2O_2 and 1000 equiv $H_2^{18}O$. [d] Percentage of alcohol with oxygen atoms coming either from H_2O_2 or H_2O. The rest is presumably originating from O_2 of atmospheric air.

$H_2^{18}O_2$ (10 equiv) in the presence of $H_2^{16}O$ (1000 equiv) indicated that the peroxide is the main source of the rest of the oxygen in the alcohol product, so that incorporation of O_2 is residual (only from 4 to 13% of oxygen atoms incorporated into alcohol products originate from air, see the mass balance in Table 3).

Interestingly, in the oxidation of tertiary C−H bonds (adamantane, DMCH, or 2,3-dimethylbutane) the extent of water incorporation into products was dramatically affected by the specific catalyst, ranging from 1% obtained with catalyst **2** to 79% with **1**. Therefore, the level of water incorporation in the oxidation of tertiary C−H bonds appears to be more sensitive to the nature of the catalyst than in the case of secondary C−H bonds.

A time course analysis of the level of ^{18}O-incorporation into cyclohexanol was studied for the oxidation of cyclohexane with H_2O_2 in the presence of $H_2^{18}O$, employing **1** and **2** as catalysts. As shown in Table 4, these analyses showed that the percentage of ^{18}O-labeled cyclohexanol remained basically constant during the whole H_2O_2 addition ((45±1)% for **1**, (15±1)% for **2**). However, the first sample taken at 5 and 14% product yield (2 equiv H_2O_2 had been added at this point) showed slightly lower values (41 and 14% ^{18}O-cyclohexanol for **1** and **2**, respectively). The analyses indicate that these reactions have an initial phase that is mechanistically distinct from the steady state. Presumably it involves a Fenton-type initial reaction of the ferrous complexes with H_2O_2, but its contribution to the overall reaction is very small and it can be practically neglected. Therefore, isotopic-labeling values measured at the end of the reactions basi-

cally reflect the steady-state mechanistic situation that exists during catalysis.

Finally, the effect of substrate concentration in the labeling results was also tested to evaluate if the competition between water exchange and reaction with the substrate took place (Table 3). Catalytic oxidation of DMCH with **1** was studied at different substrate concentrations (50–1000 mM) in the presence of $H_2^{18}O$ (1000 equiv) (see the Supporting Information, Table S2).[14b] The level of water incorporation was (82±4)% irrespective of substrate concentration. For complexes **2**, **4**, and **5**, an experiment using 50 equiv DMCH (instead of 1000 equiv as usual) in the presence of 1000 equiv $H_2^{18}O$ was performed. In all cases, the labeling results for the tertiary alcohol were essentially the same as those at higher substrate concentrations, thus indicating the absence of a competition between substrate oxidation and water exchange.

Finally, competitive oxidation of pairs of alkanes, namely DMCH and cyclohexane, was performed for catalyst **1**.[14b] In this case, the level of water incorporation into products was, within experimental error, identical to the values obtained in the single substrate oxidation experiments.

From all the data gathered from the labeling experiments, the catalysts can be classified into two different categories. On one hand, those catalysts with no substituent in the alpha position of the pyridine ring (class I: **1** and **5–10**) afforded an average value of (43±7)% of oxygen from water into cyclohexanol (2°C−H bond) and this percentage increased up to (71±8)% for tertiary C−H bonds. On the other hand, complexes with a substituent in the sixth position of the pyridine ring (class II: **2–4** and **11**) incorporated much less oxygen from water and, in contrast to the former class, the extent of water incorporation into

Table 4. Monitoring the percentage of ^{18}O-labeled cyclohexanol during the oxidation of cyclohexane by complexes **1** and **2** using H_2O_2 in the presence of $H_2^{18}O$.[a]

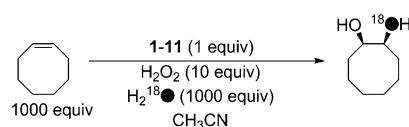| H_2O_2 [equiv]	Catalyst **1**		Catalyst **2**	
	Yield A [%]	^{18}O-labeled A [%]	Yield A [%]	^{18}O-labeled A [%]
2	5	41	14	14
4	15	44	24	15
7	30	46	44	16
10	45	46	57	15
10+10′ stirring	55	46	63	16

[a] H_2O_2 (10 equiv) was delivered by a syringe pump over a period of 30 min to an acetonitrile solution containing the iron catalyst (**1** or **2**, 1 equiv), cyclohexane (1000 equiv) and $H_2^{18}O$ (1000 equiv). The final concentrations were 1 mM catalyst, 10 mM H_2O_2, 1 M cyclohexane and 1 M $H_2^{18}O$. Aliquots were taken and analyzed at selected times after the start of H_2O_2 addition (6, 12, 21, 30, and 40 min).

tertiary C—H bonds ($7 \pm 7\%$) was smaller than in secondary ones ($19 \pm 8\%$). Thus, in contrast to our initial expectations, the sole modification of the electronic properties of the pyridine ring, which could be finely tuned by modifying the R′ substituent (γ pyridine) in Scheme 2, does not have a significant influence either in the catalytic activity of the catalyst or in the isotopic patterns of the reactions. Instead, modification of the α position of the pyridine has a profound impact in the labeling.

***cis*-Dihydroxylation of alkenes**: Complexes **1–11** can also catalyze the *cis*-dihydroxylation of alkenes by using hydrogen peroxide as the oxidant.[14a,15] For the purpose of the present work it is especially interesting to evaluate the origin of the oxygen atoms in the *cis*-dihydroxylated product, as it provides valuable information about the iron active species. Previous studies of **1**, **2**, and other non-heme iron catalysts have shown that the oxygen atoms in the *cis*-dihydroxylated product correspond to those present in the two *cis*-labile sites of the iron species responsible for the olefin *cis*-dihydroxylation event.[14a,15,17c,21,23d,f,27] Therefore, isotopic analysis of the *cis*-diol provides a molecular picture of the oxidizing species.

Consequently, under analogous reaction conditions to those detailed above for the oxidation of alkanes, we evaluated the percentage of water incorporation into the *cis*-diol product derived from the oxidation of cyclooctene (Scheme 4). For all the catalysts tested essentially only the

Scheme 4. *cis*-Dihydroxylation of cyclooctene by catalysts **1–11** using H_2O_2 as oxidant in the presence of $H_2^{18}O$.

singly labeled *cis*-diol product ($89 \pm 10\%$) was obtained (Table 5). Complementary experiments using $H_2^{18}O_2$ for catalysts **1** and **2** (as representative examples of class I and II catalysts) indicate that the second oxygen atom of the diol originates from hydrogen peroxide (see the Supporting Information, Table S3). This result further suggests that in the whole family of iron catalysts **1–11**, an iron(V)-oxo-hydroxo species containing one oxygen from water and the second one from the H_2O_2 oxidant is responsible for the observed chemistry.

Resting state of the iron species under catalytic conditions: The resting state of the iron species during C—H oxidation reactions was investigated by monitoring the catalytic oxidation of cyclohexane with complexes **1** and **2** by ESI-MS. The initial spectra of **1** and **2** in acetonitrile exhibited prominent peaks at $m/z = 453.1$ and 467.1, respectively, corresponding to $[Fe^{II}(CF_3SO_3)(L)]^+$ (L=L1 and L2) cations. Syringe-pump addition of H_2O_2 (10 equiv) to an acetonitrile solution

Table 5. Yield of *syn*-diol product and its labeling pattern in the oxidation of cyclooctene with H_2O_2 catalyzed by **1–11** in presence of $H_2^{18}O$.

Catalyst	Diol yield [%][b]	$^{16}O^{18}O$[c]
1	40	97
2	59	78
3	43	80
4	56	89
5	65	97
6	54	97
7	19	99
8	58	95
9	48	97
10	44	95
11	63	80

[a] H_2O_2 (10 equiv) was delivered by syringe pump over a period of 30 min to an acetonitrile solution containing the iron catalyst (**1–11**, 1 equiv), cyclooctene (100 equiv), and $H_2^{18}O$ (1000 equiv). The final concentrations were 1 mM catalyst, 10 mM H_2O_2, 100 mM cyclooctene, and 1 M $H_2^{18}O$. [b] Yield of diol product determined by GC. [c] Percentage of $^{16}O^{18}O$-labeled diol determined by GC-MS.

of iron catalyst (**1** or **2**) in the presence of cyclohexane resulted in the immediate consumption of the initial Fe^{II} species, as ascertained by the disappearance of the peaks corresponding to the ferrous compounds. Upon addition of 1 equiv H_2O_2, the spectra were dominated by cluster peaks at $m/z = 470.1$ and 484.1 that could be assigned to $\{[Fe^{III}(OH)(L)](CF_3SO_3)\}^+$, in which L=L1 and L2, respectively. These species remained as the major peaks in the MS spectra during the whole H_2O_2 addition.

We conclude then that ferric hydroxide species $[Fe^{III}(OH)(S)(L)]^{2+}$ constitutes the resting state during catalysis. These species are rapidly formed upon initial reaction of the ferrous complexes with H_2O_2. ESI-MS and parallel spectroscopic analyses (UV/Vis, ^1H NMR spectroscopy) do not provide direct evidence for the nature of the sixth ligand (S) that presumably binds at the ferric site to complete its likely octahedral coordination sphere. The most obvious candidates are acetonitrile solvent molecules. We infer that these are not observed in the MS experiments presumably because as they are neutral molecules, they should be relatively weakly bound to the ferric center and easily lost in the ionization process (Figure 1).

Therefore, the mechanism of the catalytic hydroxylation reaction requires consideration of the $[Fe^{III}(OH)(CH_3CN)(L)]^{2+}$ species (referred to as **Q** in Scheme 5) as the resting state, which reacts with H_2O_2 to form an oxidizing species capable of mediating stereospecific C—H bond hydroxylation.

The active species: $Fe^V(O)(OH)$: The nature of the active species in the hydroxylation reactions catalyzed by **1–11** arising from reaction of $[Fe^{III}(OH)(CH_3CN)(L)]^{2+}$ (**Q**) with H_2O_2 can be deduced from several experimental observations: 1) the mechanistic probes (selective transformations, see Table 2) and isotopic-labeling experiments (incorporation of oxygen from water into oxidized products, see Table 3) indicate that a metal-based oxidant capable of ex-
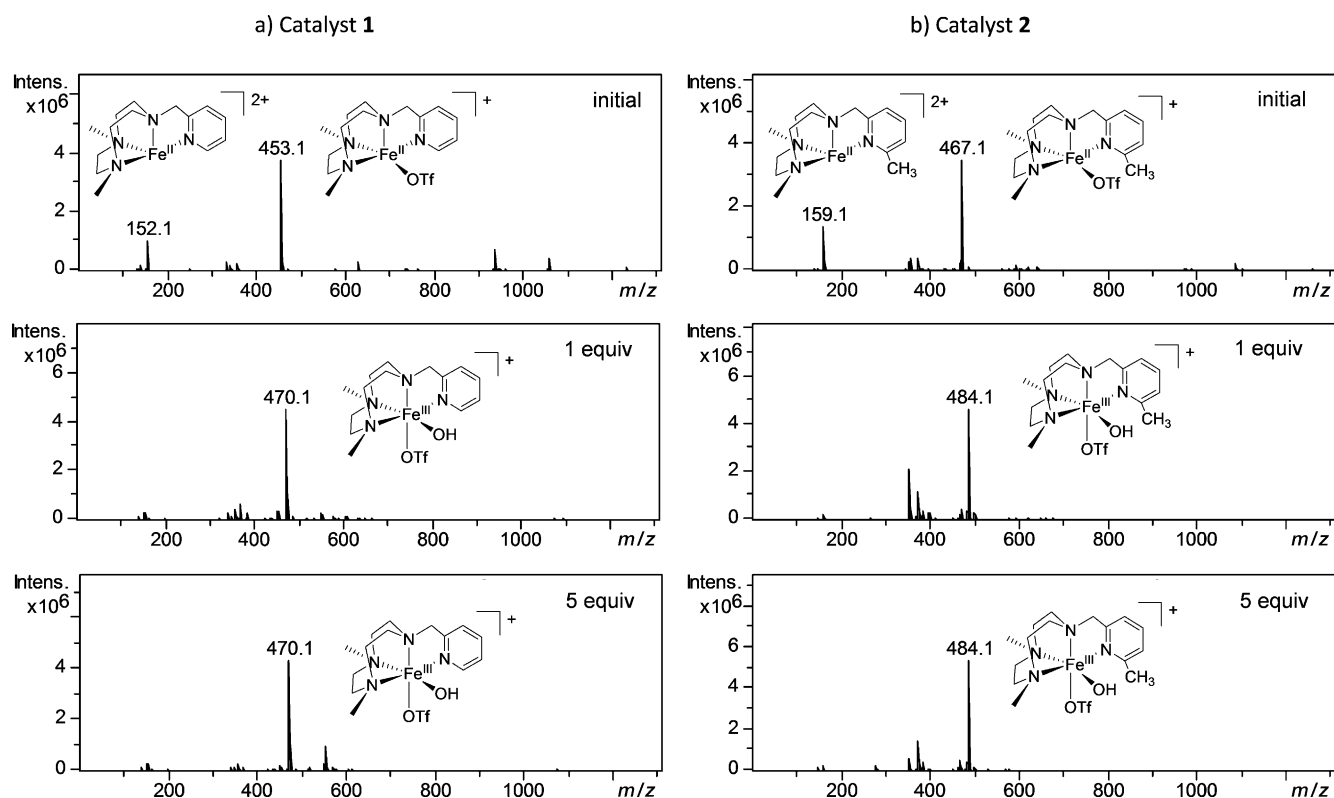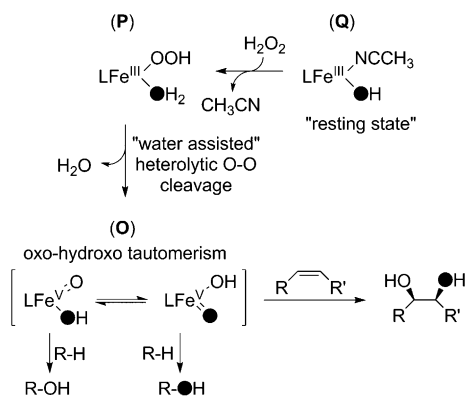
Figure 1. ESI-MS monitoring of cyclohexane oxidation by **1** and **2** under catalytic conditions (for the reaction conditions, see footnote [a] in Table 2). a) ESI-MS spectra corresponding to the reaction catalyzed by **1** before oxidant addition (top), upon addition of 1 equiv H_2O_2 (middle) and 5 equiv of H_2O_2 (bottom); b) ESI-MS spectra corresponding to the reaction catalyzed by **2** before oxidant addition (top), upon addition of 1 equiv H_2O_2 (middle) and 5 equiv of H_2O_2 (bottom).

Scheme 5. A common iron(V)-oxo-hydroxo species as the active species in C−H hydroxylation and C=C cis-dihydroxylation as postulated for [Fe-(tpa)] and [Fe(bpmen)] catalysts.
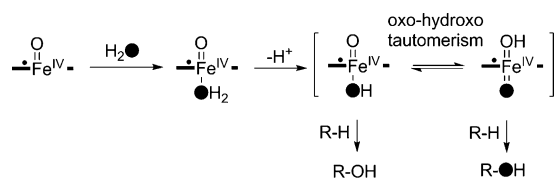
changing oxygen from water is involved. This precludes hydroxyl radicals and peroxide iron species as the C−H oxidizing agents; 2) cis-dihydroxylation of alkenes affords a cis-diol product with one oxygen atom coming from water and the other from hydrogen peroxide (see Table 5); 3) the $[Fe^{IV}(O)(S)(Pytacn)]^{2+}$ species has been recently described and it behaves as a relatively sluggish oxidant, which cannot account for the fast C−H catalytic oxidation observed;[28]

4) the $[Fe^V(O)(OH)(Pytacn)]^{2+}$ species (**O**), in which one of the oxygen atoms comes from water and the second one from the peroxide oxidant, has been recently identified from **1** by VT-MS under the same catalytic conditions used in the present work.[15] The oxygen isotopic content of these species is indicative that its formation entails a "water-assisted" heterolytic O−O cleavage in a $[Fe^{III}(OOH)(H_2O)-(Pytacn)]^{2+}$ precursor (**P**) following a mechanistic scenario reminiscent to that previously postulated by Que and co-workers (Scheme 5),[12a,17a,c,29] and that has been subsequently validated by DFT methods.[18]

The combination of these experimental facts clearly points towards the involvement of a common **O** as the active species in the hydroxylation of alkanes performed by **1–11**. However, the isotope-labeling studies for the different catalysts evidence dramatic differences in the origin of the oxygen atom that is transferred during C−H oxidation, which, in turn, suggests fundamental differences in the exact details of the C−H cleavage and/or the C−O formation event. Most significantly, these differences appear to be sensitive to the nature of the iron catalyst and the substrate.

Discrepancies with the heme paradigm: Water incorporation into oxidized products was initially studied for heme systems. It was established that it arose from the so-called oxo-hydroxo tautomerism taking place at a porphyrinic

HO−Fe=O species, involving a proton shift from the hydroxide to the terminal oxo ligand. In heme- and manganese-porphyrin systems, the oxo-hydroxo tautomerism is in competition with substrate attack (Scheme 6).[30]

Scheme 6. Oxo-hydroxo tautomerism in heme systems.

The HO−Fe=O tautomer initially formed after O−O bond-cleavage contains an oxo ligand originating from the oxidant, which is transferred to the oxidized substrate. However, through prototropic tautomerism, the initial hydroxide ligand (originated from water) becomes a terminal oxo ligand that can be subsequently transferred to the substrate. Because of the competition between tautomerism and substrate attack, the level of oxygen from water incorporated into products is inversely dependent on the concentration of substrate and on the substrate relative reactivity.[30a] In addition, the percentage of water incorporation commonly reaches a maximum value of 50%, which can be explained by considering two factors. First of all, intermolecular reaction of porphyrin HO−Fe=O species with a water molecule is slow in comparison with substrate oxidation, and thus, only intramolecular exchange takes place. A second consideration is that most porphyrins contain a plane of symmetry that render the two axial positions equivalent. Previous isotopic-labeling studies in alkane hydroxylation reactions catalyzed by non-heme complexes of the [Fe(bpmen)] and [Fe(tpa)] families (bpmen = N,N'-dimethyl-N,N'-bis(2-pyridylmethyl)ethane-1,2-diamine; tpa = tris(2-pyridylmethyl)amine) suggest that the oxo-hydroxo tautomerism is also operative for these systems (Scheme 5).[12a,17a] Indeed, the activity of these two families of catalysts accommodates to the mechanistic scenario described for porphyrinic systems in two aspects; the level of water incorporation is always less than 50%, and the percentage of oxygen from water found into products is inversely related to the strength of the oxidized C−H bond, which correlates with the corresponding ease of reactivity.[12a]

In sharp contrast, the [Fe(Pytacn)]-based catalysts studied in this work (compounds 1–11) present important discrepancies with respect to the mechanism proposed for heme systems. These discrepancies include: 1) for class I catalysts, water is the main source of oxygen atoms that end up in tertiary C−H bonds (>50%), so that these complexes cannot be strictly considered as monooxygenase type of catalysts; 2) for class I catalysts, the percentage of water incorporation is larger for substrates with weaker C−H bonds (3 °C−H > 2 °C−H); 3) the level of water incorporation is independent on substrate concentration; 4) the two positions available for interaction with the oxidant are non-equivalent and they

are disposed in a relative cis configuration; 5) the oxygen isotopic composition of the $Fe^V(O)(OH)$ intermediate in the whole family of complexes (1–11) is the same, one oxygen from water and one oxygen from H_2O_2 (see Table 5), and it is not substantially affected by exchange with external water molecules; that is, multiple exchange with water does not occur.

These observations indicate that the extent of water incorporation into products is characteristic of the nature and structure of the oxidized C−H bond and the value observed for a specific substrate does not correspond to a particular extent of the oxo-hydroxo tautomerism into the $Fe^V(O)(OH)$ species, dictated by the fastest reacting substrate. In other words, there is no competition between substrate attack and oxo-hydroxo tautomerism. This contrasts with what has been argued for the [Fe(tpa)] catalyst. Experimental data indicate that the C−H bond activation mechanism is somewhat "C−H bond dependent".
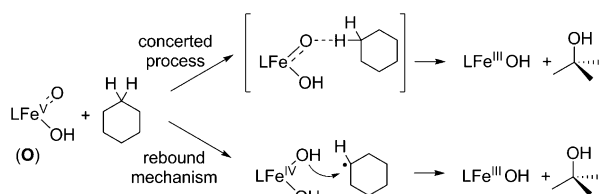
DFT calculations: To address the particular results observed in C−H hydroxylation catalyzed by [Fe(Pytacn)]-based complexes, DFT calculations were undertaken. Given the fact that our experimental observations suggest the involvement of an **O** intermediate as the active species, the general mechanistic scenario postulated for [Fe(bpmen)] and [Fe(tpa)] catalysts (Scheme 5) was taken as the reference in our calculations.[12a,17a] In particular, the hydroxylation of cyclohexane was studied in detail by using two benchmarks in the Pytacn-based compounds: complex 1 was taken as a representative of class I catalysts and complex 2 for class II catalysts. Our calculations were performed at the UB3LYP level, including both the solvent and London dispersions effects (see the Experimental Section and the Supporting Information for details).

The iron(III)-hydroxo species (**Q**) has been identified as the resting state under catalytic conditions (see above). Therefore, DFT mechanistic studies of C−H hydroxylation by 1 and 2 start with species **Q** and they finish with the formation of alcohol (Scheme 5).

In the first step, the MeCN ligand in compound **Q** is substituted by a H_2O_2 molecule, followed by a proton-transfer from the HOOH to the hydroxo ligand, leading to a low-spin iron(III)-hydroperoxo species $[Fe^{III}(OOH)(OH_2)(L)]^{2+}$ (**P**). Then, heterolytic O−O bond-cleavage of the hydroperoxo ligand, assisted by a proton from the water ligand, results in the formation of $S = 3/2$ $[Fe^V(O)(OH)(L)]^{2+}$ species (**O**), concomitant with the release of a water molecule. The water molecule formed has indeed a key role in the water-assisted rapid oxo-hydroxo tautomerism (see below). Finally, species **O** performs the hydroxylation of cyclohexane.

Careful analysis of the computational results reveals that cyclohexane hydroxylation by **O** is an asynchronous concerted process in which the hydrogen abstraction and the formation of the new C−O bond take place in a single step (Scheme 7, top). Whereas in the transition state only the hydrogen-atom abstraction can be observed (see Figure 2a), the hydroxyl rebound takes place later in the reaction path-

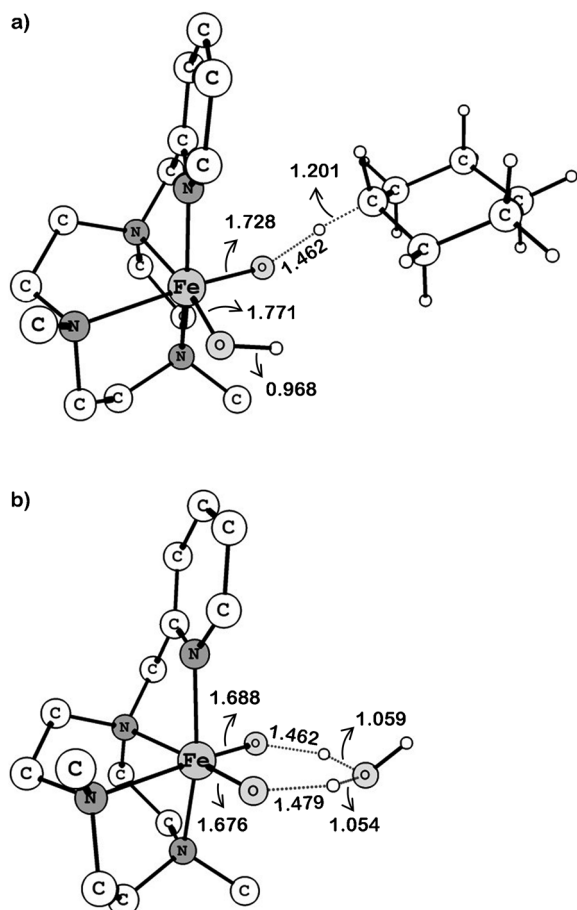Scheme 7. Two possible mechanisms for the hydroxylation of cyclohexane by **O**.

Figure 2. a) $S = 3/2$ TS corresponding to cyclohexane hydroxylation by $\mathbf{O_B}$ isomer of **1**; b) $S = 3/2$ TS corresponding to the water-assisted oxo-hydroxo tautomerism connecting $\mathbf{O_A}$ and $\mathbf{O_B}$ isomers of **1**. Hydrogen atoms have been omitted for clarity and only those relevant are depicted. Bond lengths are in Å.

way. DFT calculations show that $\{[Fe^{IV}(OH)_2(L)]^{2+}R^{\cdot}\}$ (in which $R^{\cdot}$ is a cyclohexyl radical and $L = Pytacn$ ligand) could exist as a short-lived intermediate species, because the latter is a minimum in the potential-energy landscape. Previously, this led some of us to consider that C−H hydroxylation by the **O** species was a stepwise "oxygen-rebound" mechanism (Scheme 7, bottom) involving initial hydrogen-atom transfer to form $\{[Fe^{IV}(OH)_2(L)]^{2+}R^{\cdot}\}$, followed by hydroxyl ligand rebound,[14b] such as in porphyrinic systems (Scheme 1).[6a–c] Nevertheless, intrinsic reaction coordinate (IRC) calculations have fully confirmed that the hydrogen-

atom abstraction transition-state (**TS**) directly connects **O** with the alcohol products. Thus, IRC relaxation of the transition-state geometries towards both **O** and the products rules out that the C−H hydroxylation of cyclohexane occurs through the mediation of $\{[Fe^{IV}(OH)_2(L)]^{2+}R^{\cdot}\}$.

The description of the reaction as asynchronous concerted has two very important consequences to understand the isotopic-labeling data; firstly, the alkyl radical species formed after C−H breakage has no lifetime, and because of that the reaction must proceed stereospecifically. Secondly, and most relevant to the isotopic-labeling experiments, the oxo ligand that initiates the attack over the C−H bond is the same one that ends up forming the C−OH bond. Therefore, the isotopic-labeling results must be understood as reflecting the ^{18}O-content of the oxo ligands that attack the C−H bond.

Analysis of the reaction mechanism requires consideration of the unsymmetric nature of the complexes (Scheme 8). This lack of symmetry renders the two *cis* exchangeable positions at the iron center not occupied by the tetradentate ligand (available for interaction with exogenous substrates such as the oxidant) as non-equivalent. One of the positions, labeled as A, is disposed in a relative *trans* orientation with respect to the N-CH$_2$-pyridine group, whereas the other, labeled as B, is *trans* with respect to a N-methyl group. We have designated as $\mathbf{O_A}$ the $[Fe^V(O)(OH)(L)]^{2+}$ isomer with the oxo group in position A and $\mathbf{O_B}$ the one with the oxo unit in position B. $\mathbf{O_A}$ and $\mathbf{O_B}$ also differ in the relative orientation of the pyridine ligand with respect to the Fe-oxo vector, parallel in the case of $\mathbf{O_A}$ and perpendicular in $\mathbf{O_B}$ (Figure 3). This lack of symmetry must also be considered in the preceding **Q** and **P** intermediates, which can also exist as two different isomers. Taking this into account, to rationalize our labeling results, we studied by DFT methods the above-mentioned mechanism, which starts with the resting state **Q** and leads to the final cyclohexanol product. Due to the unsymmetric nature of the complexes, the reactivities of the two isomers derived from catalysts **1** and **2** have been analyzed in detail (Scheme 8).

DFT calculations indicate that the labeling results can be explained by three key steps along the reaction mechanism: a) the relative stability of the two tautomeric $[Fe^{III}(OH)(CH_3CN)(L)]^{2+}$ isomers ($\mathbf{Q_A}$ and $\mathbf{Q_B}$), b) the oxo-hydroxo tautomerism connecting $\mathbf{O_A}$ and $\mathbf{O_B}$, and c) the activation barriers for hydrogen-atom abstraction by isomers $\mathbf{O_A}$ and $\mathbf{O_B}$.

In our calculations, the Gibbs energy of isomer $\mathbf{Q_B}$ (i.e., the one with the CH$_3$CN ligand *trans* to a N-methyl group) is lower than $\mathbf{Q_A}$ (i.e., the one with the CH$_3$CN ligand *trans* to N-CH$_2$-pyridine) by 3.76 and 2.69 kcal mol^{-1}, for **1** and **2**, respectively (see Scheme 8). As a result, $\mathbf{Q_B}$ can be considered as the catalyst resting state for both **1** and **2**, and isomer $\mathbf{P_B}$, $[Fe^{III}(OOH)_B(H_2O)_A(L)]^{2+}$, which bears the hydroperoxo ligand in position B and the water ligand (with a labeled oxygen atom in Scheme 8) in position A, is preferentially formed over $\mathbf{P_A}$ ($[Fe^{III}(OOH)_A(H_2O)_B(L)]^{2+}$).

Then, heterolytic O−O bond-cleavage of $\mathbf{P_B}$ directly gives isomer $\mathbf{O_B}$ $[Fe^V(O)_B(OH)_A(L)]^{2+}$, in which the oxo group
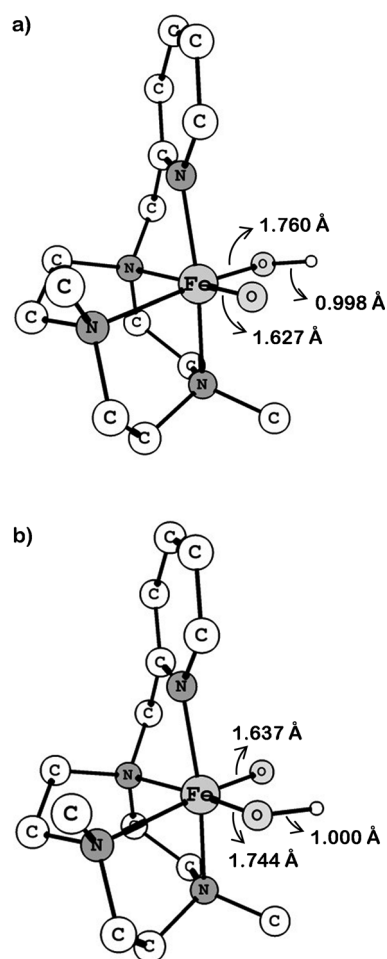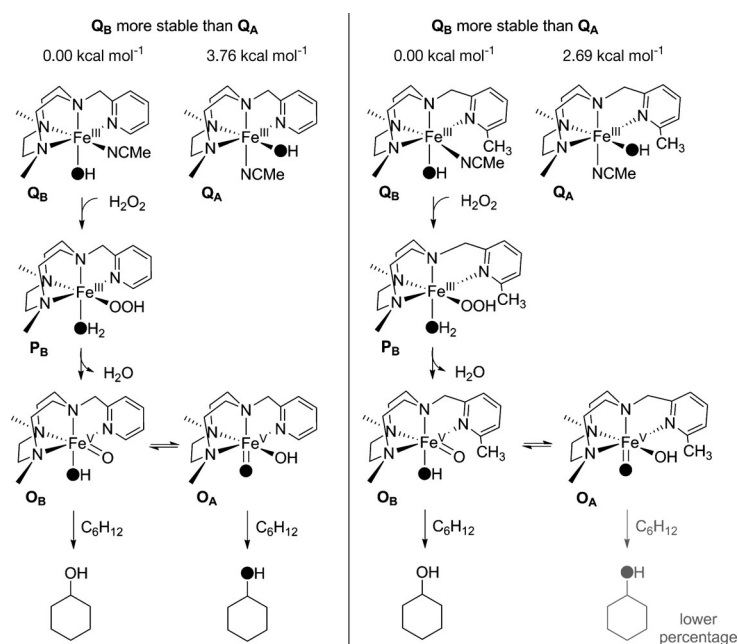
Figure 3. a) $S=3/2$ O_A isomer of 1; b) $S=3/2$ O_B isomer of 1. Hydrogen atoms have been omitted for clarity and only those relevant are depicted.

Scheme 8. Mechanism of cyclohexane hydroxylation that arises from DFT calculations considering the different isomers of catalyst 1 (left) and 2 (right).

comes from H_2O_2 and the hydroxo ligand from water. Nevertheless, we found that the two O isomers are energetically very similar, with a Gibbs energy of 0.80 and 0.55 kcal mol^{-1} in favor of isomer O_A for 1 and 2, respectively. The Gibbs energy barrier of the tautomerism between O_B and O_A is relatively small, 13.5 and 13.2 kcal mol^{-1} for 1 and 2 respectively, when the tautomerism is assisted by a water molecule (see Figure 2b), but it becomes very high in its absence (27.1 and 25.9 kcal mol^{-1} for 1 and 2, respectively). These results agree with the water-assisted barrier previously found for the Fe^V oxo-hydroxo tautomerism of the [Fe(tpa)] catalyst,[18b–d] further validating our results. It is likely that the barrier could be further lowered if more explicit water molecules were considered in the mechanism, a question that will be addressed in future studies. As a result, following the formation of O_B, a rapid oxo-hydroxo tautomerism will allow the fast interconversion with O_A, and the presence of both isomers in solution.

Thus from Q to O the mechanisms for catalyst 1 and 2 are equivalent, leading to the existence of both O_A and O_B isomers, although the oxygen that comes from the initial water ligand (i.e., the labeled oxygen in Scheme 8) is always

in the A position. This oxygen atom is the oxo ligand in O_A, but it corresponds to the hydroxo ligand in O_B.

According to this scenario, compounds 1 and 2 behave identically, leading to the same iron(V)-oxo species, with essentially identical isotopic and tautomeric composition. Consequently, differentiation leading to the experimental isotopic pattern observed in the oxidation products must arise from the next step, which involves reaction of O with the substrate.

Although cyclohexane hydroxylation by O in the doublet state ($S=1/2$) is barrierless for 1 and the O_A isomer of 2 (see Figure 4), the Gibbs energy is always higher than the quartet ($S=3/2$) transition state. Thus, we have determined the barrier of the hydroxylation step from the quartet free-energy profile. However, the doublet pathway potentially could have some role in the hydroxylation by O_A isomers, because for catalysts 1 and 2 the free energy of O_A with $S=1/2$ is only 1.0 and 2.1 kcal mol^{-1} higher than the corresponding $S=3/2$ transition state.

The hydroxylation reactivities of O_A/O_B isomer pairs for 1 and 2 are not equivalent (see Figure 4). For compound 1, isomers O_A and O_B can be considered as equally reactive because the hydroxylation of cyclohexane presents essentially the same activation barriers for hydrogen abstraction ($\Delta\Delta G^{\ddagger}=0.26$ kcal mol^{-1}). Therefore, 1 should lead to comparable amounts of ^{16}O-/^{18}O-labeled alcohols in the presence of $H_2^{18}O$, as observed in the experimental isotopic-labeling of the cyclohexanol product (Table 3).

Instead, for catalyst 2 the hydroxylation of cyclohexane performed by O_B is slightly favored over O_A ($\Delta\Delta G^{\ddagger}=2.21$ kcal mol^{-1}). This means that O_B, in which the oxo ligand
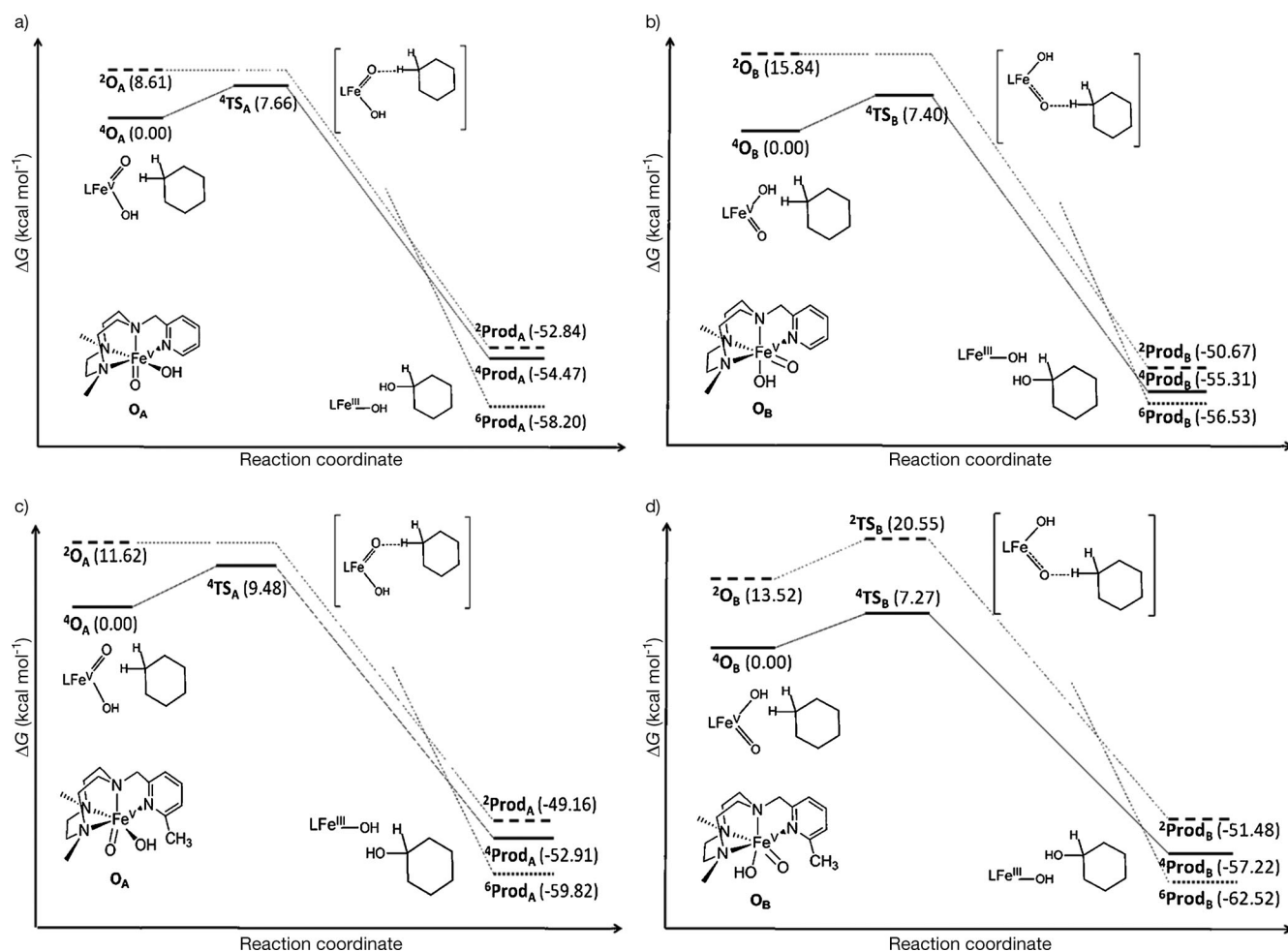
Figure 4. Free energy [kcal mol^{-1}] profiles for the concerted process of cyclohexane hydroxylation along the $S=1/2$ and $S=3/2$ potential energy surfaces by; a) O_A isomer of **1**; b) O_B isomer of **1**; c) O_A isomer of **2**; and d) O_B isomer of **2**. The most stable $S=5/2$ Fe^{III} products are also included.

originates from the oxidant (H$_2$O$_2$), dominates the C–H oxidation reaction. Again, this result agrees with the experimental labeling pattern of the cyclohexanol product obtained with catalyst **2**, which presents minimal incorporation of oxygen from water (Table 3).

The chemical basis for eliciting differential reactivity in C–H oxidation: As stated above, calculations on the mechanism of cyclohexane oxidation by **1** and **2** indicate that the relative reactivity of the O_A/O_B isomer pair in hydrogen-atom abstraction reactions is influenced by the nature of the substituent in the sixth position of the pyridine ring in the Pytacn framework. This difference in the relative reactivity provides a rationale for the markedly different isotopic-labeling patterns observed for the two classes of catalysts studied in this work.

The distinct oxidative reactivity of isomers O_A and O_B may be tentatively rationalized by taking into consideration that the two tautomers differ, among other structural aspects, in the nature of the ligand in a relative *trans* position with respect to the terminal oxo site, and in the relative orientation of the pyridine ring with respect to the Fe-oxo

vector. Indeed, both aspects have been recognized to have a defining role in the oxidative properties of high valent oxo-iron species,[17b,31] and should be considered. However, since the relative reactivities of O_A and O_B isomers appear to be more distinct in **2** than in **1**, and the relative *trans* effect is the same for both pairs, the relative orientation of the pyridine appears to be the most likely defining factor. Pyridine ligands parallel to the Fe-oxo unit place the group at α position in close proximity to the oxygen atom, and this factor has been proposed to limit reactivity by hindering the Fe=O unit from substrate approach.[31f,g,32] This analysis predicts that this factor would make O_B (Py $\perp$ Fe–O) intrinsically more reactive than O_A (Py $\parallel$ Fe–O), and that this effect would be enhanced by introducing sterically demanding groups at the α position of the pyridine. This is indeed the scenario that emerges from DFT and isotopic-labeling results.

Different reactivity of two isomeric forms of high-valent iron-oxo species finds precedent in the literature. In SyrB2 halogenases[5] and related synthetic models, halogenation or hydroxylation of the substrate occurs depending on which of the two isomers of the active Fe^{IV}(O)(Cl) species intervenes.

Computational studies by Borowski et al. of this enzyme described that the isomerization of the initially formed $Fe^{IV}(O)(Cl)$ is essential to move the chloride ligand to the most reactive position and afford halogenation of the substrate.[33] More recently, de Visser et al. studied this phenomenon employing a bioinspired model, $[Fe^{IV}(O)(tpa)(Cl)]^+$, and they also concluded that the selectivity of substrate hydroxylation versus chlorination is dependent on the stereochemistry of the oxidant.[34] In the present work, the relative reactivities of the two $[Fe^V(O)(OH)(L)]^{2+}$ isomers (O_A and O_B) are not translated into a different reaction outcome but a much subtler effect is observed, that is, markedly different levels of oxygen-atom incorporation from water. Moreover, in contrast to the hydroxylation/halogenation mechanisms in which the rebound step has a key role, calculations indicate that for [Fe(Pytacn)]-based systems hydroxylation occurs through a concerted asynchronous mechanism.

Finally, the mechanism that emerges for the stereospecific oxidation of C−H bonds by $[Fe^V(O)(OH)(Pytacn)]^{2+}$ shows fundamental differences from that operating in $[Fe^{IV}(O)(OH_2)(Pytacn)]$.[28] Most significantly, the latter behaves as a $1e^-$ oxidant and reactions are not stereospecific. Recent mechanistic and computational analyses have shown that reaction of these oxo-iron(IV) species with alkyl C−H bonds occurs through an initial hydrogen atom transfer, forming a discrete long-lived carbon-centered radical that can diffuse from the solvent cage, without engaging in hydroxyl ligand rebound.[35] These differences can be intuitively understood by considering that the Fe^{III}−OH species that form upon hydrogen abstraction must be less oxidizing than its $1e^-$ oxidized Fe^{IV}−OH counterpart. The hydroxyl ligand-rebound involves $1e^-$ reduction of the iron site and because of that it may be expected that the reaction should be disfavored as the metal site becomes less oxidizing. Therefore, in the absence of the elaborate spatial constraints imposed by enzyme active sites to control the mobility and trajectory of substrate intermediates,[36] stereospecific C−H hydroxylation appears to require a highly oxidizing $Fe^V(O)$ oxidant.

Conclusion and Final Remarks

In this work, the mechanism of C−H oxidation with H_2O_2 mediated by the [Fe(Pytacn)] family of non-heme iron catalysts has been studied by means of isotopic-labeling experiments and DFT computational methods. This family of complexes serves as a general model for the hydroxylation of an alkane with retention of the stereochemistry at a mononuclear non-heme iron center, which contains two cis-exchangeable sites. These are unique reactions that fundamentally differ from the most common Fenton-type processes because the oxidation mechanisms do not involve free-diffusing radicals. Instead, these reactions can be regarded as simple models of C−H hydroxylation reactions taking place at non-heme iron-dependent hydroxylases such as Rieske oxygenases. Isotopic analyses provide a strong support for a common $[Fe^V(O)(OH)(L)]^{2+}$ species (**O**) (L = Pytacn-based

ligand) that is formed though water-assisted O−O cleavage of a ferric-hydroperoxide species (**P**) and is responsible for C−H and C=C oxidation reactions. Most significantly, these species have been previously identified by variable temperature ESI-MS spectrometry, and shown to precede cis-dihydroxylation of an olefin.[15] In addition, analogous species have also been deduced from isotopic and computational analyses in the families of non-heme complexes [Fe-(tpa)][18b–d] and [Fe(bpmen)][12a,17c,18a] which are also competent catalysts for oxidizing C−H bonds with retention of configuration.

This work has shown that systematic manipulation of the pyridine heterocycle of the Pytacn ligand leads to two classes of non-heme iron catalysts. Class I catalysts are those in which the α position of the pyridine Pytacn ligand contains a H atom, whereas class II contain a chemical substitution at this position (Cl, F, or Me). The two families very likely operate through the same type of $[Fe^V(O)(OH)(L)]^{2+}$-oxidizing species in reactions of stereospecific C−H hydroxylation of alkanes and cis-hydroxylation of alkenes, but the two classes differ in the extent of water incorporation into alkane-oxidized products.

Differences between the two classes of catalysts could be attributed to the unsymmetric nature of the Pytacn ligand, which enforces the inequivalence of the cis-labile exchangeable sites, in which peroxide binding and terminal oxo formation occur. Two tautomeric forms of the $[Fe^V(O)(OH)(L)]^{2+}$ active species can be formed (O_A and O_B) and they are connected through fast prototopic oxo-hydroxo tautomerism. DFT computational analyses indicate that the relative reactivity of this pair of tautomers towards the C−H bonds of cyclohexane depends on the substitution at the α position of the pyridine ligand. For class I catalysts (**1** and **5–10**), tautomers O_A and O_B are equally reactive and this results in a large percentage of water incorporation into cyclohexanol (39–50%, Table 3). Instead, tautomer O_B dominates the reaction in class II catalysts, and therefore the extent of water incorporation is small. Interestingly distinct relative reactivity of O_A and O_B tautomeric species is not restricted to C−H oxidation reactions, but instead finds recent precedent in oxygen atom transfer (OAT) reactions towards olefins.[16]

DFT analyses show that the mechanism of cyclohexane oxidation entails an asynchronous concerted cleavage of the C−H bond by the $Fe^V=O$ unit, so carbon-centered radicals and Fe^{IV}−OH species cannot be considered as reaction intermediates. Consequently, the reaction is stereospecific. This also means that the oxygen atom of the oxo-ligand is the one transferred to the oxidized substrate.

Whereas the lack of intermediacy of short-lived carbon-centered intermediates in the [Fe(Pytacn)] family of non-heme catalysts could be initially considered a difference with regard to the canonical "rebound" mechanism operating in cytochrome P450 and related heme systems, recent computational analyses in the latter systems are indicative of a more subtle scenario. Shaik et al. have proposed that hydroxylation reactions by cytochrome P450 and model sys-

tems take place in a multiple spin-state reaction landscape.[6c,37] In the low spin case ($S = 1/2$ resulting from antiferromagnetic coupling between the low-spin $Fe^{IV}=O$ center and the porphyrin radical cation), the reaction of the $Fe=O$ center with a C−H bond occurs also through a concerted asynchronous mechanism, without formation of discrete intermediates. In contrast, the high-spin state ($S = 3/2$ resulting from ferromagnetic coupling) involves sequential C−H breakage, with formation of carbon-centered radicals, with a significant lifetime before hydroxyl rebound from the Fe^{IV}−OH site takes place. Computational analyses in the present family of complexes do not provide evidence for a multiple spin-state scenario, but the experimental results are reminiscent of the low-spin scenario proposed in cytochrome P450 and account for a stereospecific C−H hydroxylation mechanism. Furthermore, previous computational analyses of the reaction mechanism for C−H oxidation by the [Fe(tpa)] family of catalysts[18b–d] also agree with our analyses for the [Fe(Pytacn)] family.

In conclusion, this work provides an understanding of the reaction mechanism of C−H oxidation by non-heme species that serve as functional models for non-heme oxygenase enzymes. Stereospecific C−H oxidation by these non-heme sites shares fundamental aspects with the reaction mechanism taking place at heme sites. However, the presence of cis-exchangeable sites introduces a richer mechanistic versatility that opens up new reaction paths that warrant further exploration.

Experimental Section

Reaction conditions for catalysis: In a typical reaction 0.36 mL of a 70 mm (25 μmol) H_2O_2 solution (diluted from a 35 % H_2O_2 aqueous solution) together with H_2O (45 μL, 2500 μmol) in CH_3CN was delivered by syringe pump over 30 min at 25 °C in air to a vigorously stirred CH_3CN solution (2.14 mL) containing the iron catalyst (2.5 μmol) and the alkane substrate (2500 μmol). The final concentrations of reagents were 1 mm iron catalyst, 10 mm H_2O_2, 1 m H_2O and 1 m substrate. For adamantane, due to low solubility, only 25 μmol of substrate were added and so the final concentration was 10 mm for this substrate. After syringe-pump addition, the resulting solution was stirred for another 10 min. Biphenyl was added at this point as an internal standard. The iron complex was removed by passing the solution through a short path of silica followed by elution with of ethyl acetate (2 mL). Finally, the solution was subjected to GC analysis. The organic products were identified by comparison with authentic compounds. For the measurement of kinetic isotope effect (KIE), a substrate mixture of cyclohexane/[D_{12}]cyclohexane (1:3) was used to improve the accuracy of the KIE values obtained. For the oxidation of cyclooctene, the reactions were performed as described above but using 250 μmol of substrate. However, after syringe-pump addition and stirring for 10 min, the reaction mixture was subjected to a pretreatment. Acetic anhydride (1 mL) together with 1-methylimidazole (0.1 mL) were added to afford the esterification of the diol product. After stirring for 15 min at room temperature, ice was added and the mixture was stirred for about 30 min. Biphenyl (internal standard) was added at this point and the mixture was extracted with $CHCl_3$ (2 mL). The organic layer was washed with 1 m H_2SO_4 (2 mL), sat. $NaHCO_3$ (2 mL) and H_2O (2 mL), dried with $MgSO_4$ and subjected to GC analysis. The organic products were identified by comparison with authentic compounds.

Isotope-labeling studies: *Reaction catalytic conditions using $H_2^{18}O$*: In a typical reaction, 0.29 mL of a 70 mm (20 μmol) H_2O_2 solution (diluted

from a 35 % H_2O_2 aqueous solution) together with 40 μL of $H_2^{18}O$ (2000 μmol) in CH_3CN was delivered by syringe pump over 30 min at 25 °C in air to a vigorously stirred CH_3CN solution (1.71 mL) containing the iron catalyst (2.0 μmol) and the alkane substrate (2000 μmol). The final concentrations of reagents were 1 mm iron catalyst (**1–11**), 10 mm H_2O_2, 1 m $H_2^{18}O$/32 mm $H_2^{16}O$ and 1 m substrate. For adamantane, due to low solubility, only 200 μmol of substrate were added and so the final concentration was 10 mm for this substrate. For cyclooctene only 200 μmol of substrate were added and so the final concentration was 100 mm for this substrate. After syringe pump addition, the resulting solution was stirred for another 10 min.

Reaction catalytic conditions using $H_2^{18}O_2$: In a typical reaction, 0.29 mL of a 70 mm (20 μmol) $H_2^{18}O_2$ solution (diluted from a 2 % $H_2^{18}O_2$ aqueous solution) in CH_3CN was delivered by syringe pump over 30 min at 25 °C in air to a vigorously stirred CH_3CN solution (1.71 mL) containing the iron catalyst (2.0 μmol) and the alkane substrate (2000 μmol). The final concentrations of reagents were 1 mm iron catalyst (**1**), 10 mm $H_2^{18}O_2$, 1 m H_2O and 1 m substrate. For adamantane, due to low solubility, only 20 μmol of substrate were added and so the final concentration was 10 mm for this substrate. For cyclooctene only 20 μmol of substrate were added and so the final concentration was 100 mm for this substrate. After syringe-pump addition, the resulting solution was stirred for another 10 min.

Preparation of the samples for GC-MS analyses: In the oxidation of adamantane, cis-1,2-dimethylcyclohexane and 2,3-dimethylbutane the reaction mixture was directly passed through a short path of silica to remove the iron catalyst followed by elution with ethyl acetate (2 mL). For cyclohexane and cyclooctene, the reaction solutions were treated with 1-methylimidazole (0.1 mL) and acetic anhydride (1 mL) to esterify the alcohol products following the protocol described above (tertiary alcohols were not esterified under these conditions).

Analysis of the isotopic data: Isotopic composition of the products was obtained by GC-MS analyses using a chemical ionization mode with a 50 % NH_3/CH_4 mix as the ionization gas. The ^{18}O-content of the final alcohol and diol products (or their esterified analogues when applicable) was determined by the relative abundances of the ^{18}O-labeled with respect to the ^{16}O-labeled product. The peak corresponding to the molecular mass plus ammonium $[M + NH_4]$ was used to determine the isotopic content. The $[M + NH_4]$ peaks corresponding to the alcohols or syn-diol products were computer-simulated to determine their [18]O isotopic content. The following corrections were applied to the simulations to account for the isotopic purity of $H_2^{18}O$ and $H_2^{18}O_2$ and also for the dilution of $H_2^{18}O$ due to the use of aqueous H_2O_2 solutions: a) In reactions run in the presence of $H_2^{18}O$ (1 m, 98 % ^{18}O-enriched), corrected values were obtained by dividing the simulated percentage of ^{18}O-labeled alcohol and [16]O[18]O-labeled syn-diol by 0.94; b) In reactions run with $H_2^{18}O_2$ (10 mm, 90 % ^{18}O-enriched), corrected values were obtained by dividing the simulated percentage of ^{18}O-labeled alcohol by 0.90.

Computational details: DFT geometries were optimized at the UB3LYP level in conjunction with the SDD basis set and associated ECP for Fe, and the 6–311G(d,p) basis for the other atoms, as implemented in the Gaussian 09 program.[38] The energies were further refined by single point calculations by using cc-pVTZ basis set. Enthalpic and free energy corrections were computed at the UB3LYP/SDD&6–311G(d,p) level. The final free energies also include acetonitrile solvent effect computed through PCM-SMD approach and London dispersion effects calculated using the S. Grimme DFT-D3 method. The connections between the transition states and minimums in energy of the pathway were checked by IRC calculations (see the Supporting Information for further details and full reference).

FULL PAPER

[1] a) *Handbook of C−H Transformations, Vol. 1−2* (Ed.: G. Dyker), Wiley-VCH, Weinheim, **2005**; b) C.-L. Sun, B.-J. Li, Z.-J. Shi, *Chem. Rev.* **2011**, *111*, 1293–1314; c) T. Newhouse, P. S. Baran, *Angew. Chem. Int. Ed.* **2011**, *50*, 3362–3374; d) L. McMurray, F. O'Hara, M. J. Gaunt, *Chem. Soc. Rev.* **2011**, *40*, 1885–1898; e) G. B. Shul′pin, *Org. Biomol. Chem.* **2010**, *8*, 4217–4228.

[2] *Modern Oxidation Methods* (Ed.: J.-E. Bäckvall), Wiley-VCH, Weinheim, **2004**.

[3] a) A. Correa, O. G. Mancheño, C. Bolm, *Chem. Soc. Rev.* **2008**, *37*, 1108–1117; b) S. Enthaler, K. Junge, M. Beller, *Angew. Chem.* **2008**, *120*, 3363–3367; *Angew. Chem. Int. Ed.* **2008**, *47*, 3317–3321; c) L.-X. Liu, *Curr. Org. Chem.* **2010**, *14*, 1099–1126; d) E. B. Bauer, *Curr. Org. Chem.* **2008**, *12*, 1341–1369; e) *Iron Catalysis in Organic Chemistry* (B. Plietker), Wiley-VCH, Weinheim, **2008**.

[4] *Cytochrome P450: Structure, Mechanism and Biochemistry*, 3rd ed. (Ed.: P. R. Ortiz de Montellano,), Kluwer Academic/Plenum Publishers, New York, **2005**.

[5] a) E. G. Kovaleva, J. D. Lipscomb, *Nat. Chem. Biol.* **2008**, *4*, 186–193; b) M. M. Abu-Omar, A. Loaiza, N. Hontzeas, *Chem. Rev.* **2005**, *105*, 2227–2252; c) P. C. A. Bruijnincx, G. v. Koten, R. J. M. K. Gebbink, *Chem. Soc. Rev.* **2008**, *37*, 2716–2744; d) E. Y. Tshuva, S. J. Lippard, *Chem. Rev.* **2004**, *104*, 987–1012; e) M. Costas, M. P. Mehn, M. P. Jensen, L. Que, Jr., *Chem. Rev.* **2004**, *104*, 939–986.

[6] a) S. Shaik, S. Cohen, Y. Wang, H. Chen, D. Kumar, W. Thiel, *Chem. Rev.* **2010**, *110*, 949–1017; b) P. R. Ortiz de Montellano, *Chem. Rev.* **2010**, *110*, 932–948; c) B. Meunier, S. P. de Visser, S. Shaik, *Chem. Rev.* **2004**, *104*, 3947–3980; d) I. Schlichting, J. Berendzen, K. Chu, A. M. Stock, S. A. Maves, D. E. Benson, R. M. Sweet, D. Ringe, G. A. Petsko, S. G. Sligar, *Science* **2000**, *287*, 1615–1622.

[7] J. T. Groves, G. A. McClusky, R. E. White, M. J. Coon, *Biochem. Biophys. Res. Commun.* **1978**, *81*, 154–160.

[8] a) M. D. Wolfe, J. V. Parales, D. T. Gibson, J. D. Lipscomb, *J. Biol. Chem.* **2001**, *276*, 1945–1953; b) S. Chakrabarty, R. N. Austin, D. Deng, J. T. Groves, J. D. Lipscomb, *J. Am. Chem. Soc.* **2007**, *129*, 3514–3515.

[9] a) C.-M. Che, V. K.-Y. Lo, C.-Y. Zhou, J.-S. Huang, *Chem. Soc. Rev.* **2011**, *40*, 1950–1975; b) M. Costas, *Coord. Chem. Rev.* **2011**, *255*, 2912–2932; c) A. Robert, B. Meunier in *Biomimetic Oxidations Catalyzed by Transition-Metal Complexes* (Ed.: B. Meunier), Imperial College Press, London, **2000**, pp. 543–562; d) B. Meunier, *Chem. Rev.* **1992**, *92*, 1411–1456; e) W. Nam, *Acc. Chem. Res.* **2007**, *40*, 522–531; f) J. T. Groves in *Cytochrome P450: Structure, Mechanism and Biochemistry*, 3rd ed. (Ed.: P. R. Ortiz de Montellano), Kluwer Academic/Plenum Publishers, New York, **2005**, pp. 1–42.

[10] L. Que, Jr., W. B. Tolman, *Nature* **2008**, *455*, 333–340.

[11] M. Costas, K. Chen, L. Que, Jr., *Coord. Chem. Rev.* **2000**, *200–202*, 517–544.

[12] a) K. Chen, L. Que, Jr., *J. Am. Chem. Soc.* **2001**, *123*, 6327–6337; b) C. Kim, K. Chen, J. Kim, L. Que, Jr., *J. Am. Chem. Soc.* **1997**, *119*, 5964–5965.

[13] a) M. C. White, *Science* **2012**, *335*, 807–809; b) Y. Hitomi, K. Arakawa, T. Funabiki, M. Kodera, *Angew. Chem. Int. Ed.* **2012**, *51*, 3448–3452; c) P. Liu, Y. Liu, E. L.-M. Wong, S. Xiang, C.-M. Che, *Chem. Sci.* **2011**, *2*, 2187–2195; d) L. Gómez, I. Garcia-Bosch, A. Company, J. Benet-Buchholz, A. Polo, X. Sala, X. Ribas, M. Costas, *Angew. Chem.* **2009**, *121*, 5830–5833; *Angew. Chem. Int. Ed.* **2009**, *48*, 5720–5723; e) M. A. Bigi, S. A. Reed, M. C. White, *J. Am. Chem. Soc.* **2012**, *134*, 9721–9726; f) M. A. Bigi, S. A. Reed, M. C. White, *Nat. Chem.* **2011**, *3*, 218; g) M. S. Chen, M. C. White, *Science* **2010**, *327*,

566–571; h) N. A. Vermeulen, M. S. Chen, M. C. White, *Tetrahedron* **2009**, *65*, 3078–3084; i) M. S. Chen, M. C. White, *Science* **2007**, *318*, 783–787.

[14] a) A. Company, L. Gómez, X. Fontrodona, X. Ribas, M. Costas, *Chem. Eur. J.* **2008**, *14*, 5727–5731; b) A. Company, L. Gómez, M. Güell, X. Ribas, J. M. Luis, L. Que, Jr., M. Costas, *J. Am. Chem. Soc.* **2007**, *129*, 15766–15767.

[15] I. Prat, J. S. Mathieson, M. Güell, X. Ribas, J. M. Luis, L. Cronin, M. Costas, *Nat. Chem.* **2011**, *3*, 788–793.

[16] A. Company, Y. Feng, M. Güell, X. Ribas, J. M. Luis, L. Que, Jr., M. Costas, *Chem. Eur. J.* **2009**, *15*, 3359–3362.

[17] a) K. Chen, L. Que, Jr., *Chem. Commun.* **1999**, 1375–1376; b) M. Costas, L. Que, Jr., *Angew. Chem.* **2002**, *114*, 2283–2285; *Angew. Chem. Int. Ed.* **2002**, *41*, 2179–2181; c) K. Chen, M. Costas, J. Kim, A. K. Tipton, L. Que, Jr., *J. Am. Chem. Soc.* **2002**, *124*, 3026–3035; d) S. H. Lee, J. H. Han, H. Kwak, S. J. Lee, E. Y. Lee, H. J. Kim, J. H. Lee, C. Bae, S. N. Lee, Y. Kim, C. Kim, *Chem. Eur. J.* **2007**, *13*, 9393–9398; e) J. Yoon, S. A. Wilson, Y. K. Jang, M. S. Seo, K. Nehru, B. Hedman, K. O. Hodgson, E. Bill, E. I. Solomon, W. Nam, *Angew. Chem.* **2009**, *121*, 1283–1286; *Angew. Chem. Int. Ed.* **2009**, *48*, 1257–1260; f) P. Das, L. Que, Jr., *Inorg. Chem.* **2010**, *49*, 9479–9485.

[18] a) D. Quiñonero, K. Morokuma, D. G. Musaev, R. Mas-Balleste, L. Que, Jr., *J. Am. Chem. Soc.* **2005**, *127*, 6548–6549; b) A. Bassan, R. A. M. Blomberg, E. M. P. Siegbahn, L. Que, Jr., *Chem. Eur. J.* **2005**, *11*, 692–705; c) A. Bassan, R. A. M. Blomberg, E. M. P. Siegbahn, L. Que, Jr., *Angew. Chem.* **2005**, *117*, 2999–3001; *Angew. Chem. Int. Ed.* **2005**, *44*, 2939–2941; d) A. Bassan, M. R. A. Blomberg, P. E. M. Siegbahn, L. Que, Jr., *J. Am. Chem. Soc.* **2002**, *124*, 11056–11063.

[19] O. V. Makhlynets, E. V. Rybak-Akimova, *Chem. Eur. J.* **2010**, *16*, 13995–14006.

[20] a) O. Y. Lyakin, R. V. Ottenbacher, K. P. Bryliakov, E. P. Talsi, *ACS Catal.* **2012**, *2*, 1196–1202; b) O. Y. Lyakin, K. P. Bryliakov, E. P. Talsi, *Inorg. Chem.* **2011**, *50*, 5526–5538; c) O. Y. Lyakin, K. P. Bryliakov, G. J. P. Britovsek, E. P. Talsi, *J. Am. Chem. Soc.* **2009**, *131*, 10798–10799; d) O. Y. Lyakin, I. Prat, K. P. Bryliakov, M. Costas, E. P. Talsi, *Catal. Commun.* **2012**, *29*, 105–108.

[21] T. W.-S. Chow, E. L.-M. Wong, Z. Guo, Y. Liu, J.-S. Huang, C.-M. Che, *J. Am. Chem. Soc.* **2010**, *132*, 13229–13239.

[22] a) K. M. Van Heuvelen, A. T. Fiedler, X. Shan, R. F. De Hont, K. K. Meier, E. L. Bominaar, E. Muenck, L. Que, Jr., *Proc. Natl. Acad. Sci. USA* **2012**, *109*, 11933–11938; b) F. T. de Oliveira, A. Chanda, D. Banerjee, X. Shan, S. Mondal, L. Que, Jr., E. L. Bominaar, E. Münck, T. J. Collins, *Science* **2007**, *315*, 835–838.

[23] a) P. Comba, M. Maurer, P. Vadivelu, *Inorg. Chem.* **2009**, *48*, 10389–10396; b) P. Comba, G. Rajaraman, H. Rohwer, *Inorg. Chem.* **2007**, *46*, 3826–3838; c) J. Bautz, P. Comba, C. L. d. Laorden, M. Menzel, G. Rajaraman, *Angew. Chem.* **2007**, *119*, 8213–8216; *Angew. Chem. Int. Ed.* **2007**, *46*, 8067–8070; d) M. R. Bukowski, P. Comba, A. Lienke, C. Limberg, C. L. de Laorden, R. Mas-Balleste, M. Merz, L. Que, Jr., *Angew. Chem.* **2006**, *118*, 3524–3528; *Angew. Chem. Int. Ed.* **2006**, *45*, 3446–3449; e) M. R. Bukowski, P. Comba, C. Limberg, M. Merz, L. Que, Jr., T. Wistuba, *Angew. Chem.* **2004**, *116*, 1303–1307; *Angew. Chem. Int. Ed.* **2004**, *43*, 1283–1287; f) P. D. Oldenburg, Y. Feng, I. Pryjomska-Ray, D. Ness, L. Que, Jr., *J. Am. Chem. Soc.* **2010**, *132*, 17713–17723; g) A. Thibon, V. Jollet, C. Ribal, K. Senechal-David, L. Billon, A. B. Sorokin, F. Banse, *Chem. Eur. J.* **2012**, *18*, 2715–2724.

[24] a) Y. Zang, J. Kim, Y. Dong, E. C. Wilkinson, E. H. Appelman, L. Que, Jr., *J. Am. Chem. Soc.* **1997**, *119*, 4197–4205; b) E. C. Constable, G. Baum, E. Bill, R. Dyson, R. v. Eldik, D. Fenske, S. Kaderli, D. Morris, A. Neubrand, M. Neuburger, D. R. Smith, K. Wieghardt, M. Zehnder, A. D. Zuberbühler, *Chem. Eur. J.* **1999**, *5*, 498–508.

[25] a) J. England, R. Gondhia, L. Bigorra-Lopez, A. R. Petersen, A. J. P. White, G. J. P. Britovsek, *Dalton Trans.* **2009**, 5319–5334; b) J. England, C. R. Davies, M. Banaru, A. J. P. White, G. J. P. Britovsek, *Adv. Synth. Catal.* **2008**, *350*, 883–897; c) J. England, G. J. P. Britovsek, N. Rabadia, A. J. P. White, *Inorg. Chem.* **2007**, *46*, 3752–3767;

d) G. J. P. Britovsek, J. England, A. J. P. White, *Inorg. Chem.* **2005**, *44*, 8125–8134; e) A. Company, L. Gomez, M. Costas in *Iron-Containing Enzymes: Versatile Catalysts of Hydroxylation Reactions in Nature* (Eds.: S. P. De Visser, D. Kumar), RSC, Cambridge, **2011**; f) G. Roelfes, M. Lubben, R. Hage, L. Que, Jr., B. L. Feringa, *Chem. Eur. J.* **2000**, *6*, 2152–2159.

[26] K. U. Ingold, P. A. MacFaul in *Biomimetic Oxidations Catalyzed by Transition-Metal Complexes* (Ed.: B. Meunier), Imperial College Press, London, **2000**, pp. 45–89.

[27] a) P. Comba, G. Rajaraman, *Inorg. Chem.* **2008**, *47*, 78–93; b) Y. Feng, J. England, L. Que, Jr., *ACS Catal.* **2011**, *1*, 1035–1042.

[28] A. Company, I. Prat, J. R. Frisch, R. M. Ballesté, M. Güell, G. Juhász, X. Ribas, E. Münck, J. M. Luis, L. Que, Jr., M. Costas, *Chem. Eur. J.* **2011**, *17*, 1622–1634.

[29] K. Chen, M. Costas, L. Que, Jr., *J. Chem. Soc. Dalton Trans.* **2002**, 672–679.

[30] a) J. Bernadou, B. Meunier, *Chem. Commun.* **1998**, 2167–2173; b) J. Bernadou, A.-S. Fabiano, A. Robert, B. Meunier, *J. Am. Chem. Soc.* **1994**, *116*, 9375–9376; c) W. Nam, M. H. Lim, S. K. Moon, C. Kim, *J. Am. Chem. Soc.* **2000**, *122*, 10805–10809.

[31] a) Y. Kang, H. Chen, Y. J. Jeong, W. Lai, E. H. Bae, S. Shaik, W. Nam, *Chem. Eur. J.* **2009**, *15*, 10039–10046; b) S. P. de Visser, L. Tahsini, W. Nam, *Chem. Eur. J.* **2009**, *15*, 5577–5587; c) T. A. Jackson, J. U. Rohde, M. S. Seo, C. V. Sastri, R. DeHont, A. Stubna, T. Ohta, T. Kitagawa, E. Munck, W. Nam, L. Que, Jr., *J. Am. Chem. Soc.* **2008**, *130*, 12394–12407; d) H. Hirao, L. Que, Jr., W. Nam, S. Shaik, *Chem. Eur. J.* **2008**, *14*, 1740–1756; e) C. V. Sastri, J. Lee, K. Oh, Y. J. Lee, J. Lee, T. A. Jackson, K. Ray, H. Hirao, W. Shin, J. A. Halfen, J. Kim, L. Que, Jr., S. Shaik, W. Nam, *Proc. Natl. Acad. Sci. USA* **2007**, *104*, 19181–19186; f) D. Wang, K. Ray, M. J. Collins, E. R. Farquhar, J. R. Frisch, L. Gómez, T. A. Jackson, M. Kerscher, A. Waleska, P. Comba, M. Costas, L. Que, Jr., *Chem. Sci.* **2013**, *4*, 282–291; g) S. D. Wong, C. B. Bell, III, L. V. Liu, Y. Kwak, J. England, E. E. Alp, J. Zhao, L. Que, Jr., E. I. Solomon, *Angew. Chem.* **2011**, *123*, 3273–3276; *Angew. Chem. Int. Ed.* **2011**, *50*, 3215–3218; h) S. Hong, Y.-M. Lee, K.-B. Cho, K. Sundaravel, J. Cho, M. J. Kirn, W. Shin, W. Nam, *J. Am. Chem. Soc.* **2011**, *133*, 11876–11879.

[32] A. R. McDonald, Y. Guo, V. V. Vu, E. L. Bominaar, E. Münck, L. Que, Jr., *Chem. Sci.* **2012**, *3*, 1680–1693.

[33] T. Borowski, H. Noack, M. Radoń, K. Zych, P. E. M. Siegbahn, *J. Am. Chem. Soc.* **2010**, *132*, 12887–12898.

[34] M. Quesne, S. Visser, *J. Biol. Inorg. Chem.* **2012**, *17*, 841–852.

[35] K.-B. Cho, X. Wu, Y.-M. Lee, Y. H. Kwon, S. Shaik, W. Nam, *J. Am. Chem. Soc.* **2012**, *134*, 20222–20225.

[36] a) R. N. Austin, K. Luddy, K. Erickson, M. Pender-Cudlip, E. Bertrand, D. Deng, R. S. Buzdygon, J. B. v. Beilen, J. T. Groves, *Angew. Chem.* **2008**, *120*, 5310–5312; *Angew. Chem. Int. Ed.* **2008**, *47*, 5232–5234; b) M. L. Matthews, C. S. Neumann, L. A. Miles, T. L. Grove, S. J. Booker, C. Krebs, C. T. Walsh, J. M. Bollinger, Jr., *Proc. Natl. Acad. Sci. USA* **2009**, *106*, 17723–17728.

[37] a) S. Shaik, D. Kumar, S. P. de Visser, A. Altun, W. Thiel, *Chem. Rev.* **2005**, *105*, 2279–2328; b) S. Shaik, S. Cohen, S. P. de Visser, P. K. Sharma, D. Kumar, S. Kozuch, F. Ogliaro, D. Danovich, *Eur. J. Inorg. Chem.* **2004**, *2*, 207–226; c) F. Ogliaro, N. Harris, S. Cohen, M. Filatov, S. P. deVisser, S. Shaik, *J. Am. Chem. Soc.* **2000**, *122*, 8977–8989.

[38] Gaussian 09, Revision A.02, M. J. Frisch, G. W. Trucks, H. B. Schlegel, G. E. Scuseria, M. A. Robb, J. R. Cheeseman, G. Scalmani, V. Barone, B. Mennucci, G. A. Petersson, H. Nakatsuji, M. Caricato, X. Li, H. P. Hratchian, A. F. Izmaylov, J. Bloino, G. Zheng, J. L. Sonnenberg, M. Hada, M. Ehara, K. Toyota, R. Fukuda, J. Hasegawa, M. Ishida, T. Nakajima, Y. Honda, O. Kitao, H. Nakai, T. Vreven, J. A. Montgomery, Jr., J. E. Peralta, F. Ogliaro, M. Bearpark, J. J. Heyd, E. Brothers, K. N. Kudin, V. N. Staroverov, R. Kobayashi, J. Normand, K. Raghavachari, A. Rendell, J. C. Burant, S. S. Iyengar, J. Tomasi, M. Cossi, N. Rega, J. M. Millam, M. Klene, J. E. Knox, J. B. Cross, V. Bakken, C. Adamo, J. Jaramillo, R. Gomperts, R. E. Stratmann, O. Yazyev, A. J. Austin, R. Cammi, C. Pomelli, J. W. Ochterski, R. L. Martin, K. Morokuma, V. G. Zakrzewski, G. A. Voth, P. Salvador, J. J. Dannenberg, S. Dapprich, A. D. Daniels, O. Farkas, J. B. Foresman, J. V. Ortiz, J. Cioslowski, D. J. Fox, Gaussian, Inc., Wallingford CT, **2009**.